Endogenous growth factor stimulation of hemocyte proliferation induces resistance to *Schistosoma mansoni* challenge in the snail host

Emmanuel A. Pila[a], Michelle A. Gordy[a], Valerie K. Phillips[a], Alethe L. Kabore[a], Sydney P. Rudko[a], and Patrick C. Hanington[a,1]

[a]School of Public Health, University of Alberta, Edmonton, AB, Canada T6G2G7

Digenean trematodes are a large, complex group of parasitic flatworms that infect an incredible diversity of organisms, including humans. Larval development of most digeneans takes place within a snail (Gastropoda). Compatibility between snails and digeneans is often very specific, such that suitable snail hosts define the geographical ranges of diseases caused by these worms. The immune cells (hemocytes) of a snail are sentinels that act as a crucial barrier to infection by larval digeneans. Hemocytes coordinate a robust and specific immunological response, participating directly in parasite killing by encapsulating and clearing the infection. Hemocyte proliferation and differentiation are influenced by unknown digenean-specific exogenous factors. However, we know nothing about the endogenous control of hemocyte development in any gastropod model. Here, we identify and functionally characterize a progranulin [*Biomphalaria glabrata* granulin (*Bg*GRN)] from the snail *B. glabrata*, a natural host for the human blood fluke *Schistosoma mansoni*. Granulins are growth factors that drive proliferation of immune cells in organisms, spanning the animal kingdom. We demonstrate that *Bg*GRN induces proliferation of *B. glabrata* hemocytes, and specifically drives the production of an adherent hemocyte subset that participates centrally in the anti-digenean defense response. Additionally, we demonstrate that susceptible *B. glabrata* snails can be made resistant to infection with *S. mansoni* by first inducing hemocyte proliferation with *Bg*GRN. This marks the functional characterization of an endogenous growth factor of a gastropod mollusc, and provides direct evidence of gain of resistance in a snail-digenean infection model using a defined factor to induce snail resistance to infection.

Biomphalaria glabrata | *Schistosoma mansoni* | schistosomiasis | granulin | hematopoiesis

Snails of the genus *Biomphalaria* serve as the intermediate host for *Schistosoma mansoni*, one of the species of parasitic flatworms that cause schistosomiasis. The extensive amplification of the parasite within the snail host complicates disease control efforts and is one of the reasons that schistosomiasis continues to be one of the most important neglected tropical diseases. Studies investigating compatibility between *Biomphalaria* snails and *S. mansoni* suggest that the snail immune response plays a crucial role in determining infection outcome. Although circulating humoral factors are known to play an important role in determining infection outcome via recognition of various parasite targets, or by directly damaging the parasite tegument (1–4), it is ultimately the immune cells of the snail, known as hemocytes, that are primarily responsible for encapsulating and eliminating the parasite (5).

The central role of hemocytes in the anti-schistosome response underscores the importance of maintaining suitable numbers of circulating and tissue-resident immune cells. We currently understand very little about the mechanics of hematopoiesis in gastropods. Our limited understanding of the process suggests that the primary hematopoietic organ in snails is a thin tissue located in the anterior of the pericardial region known as the amoebocyte-producing organ (APO) (6). Following stimulation with excretory/

secretory (ES) products of digenean trematodes, such as *S. mansoni* (7) or *Echinostoma paraensei* (8), the APO noticeably swells and displays an increase in mitotic events (9). The hemocytes generated during these events tend to be adherent and granulocytic, and exhibit greater capacity to generate humoral factors relevant to parasite killing compared with the preexisting population (2). Following the stimulation of hemocyte development by exogenous factors, the proportion of hemocyte subsets alters to favor the granulocytic morphology (9) that is typically associated with parasite encapsulation (10), phagocytosis (2), and the production of reactive oxygen and nitrogen intermediates (11) important for parasite killing.

Parasite-specific factors that are excreted or secreted upon initial infection of the snail are important drivers of hematopoiesis in *B. glabrata*. The second, and lesser-understood, drivers are endogenous snail growth factors that, in response to infection, induce hemocyte proliferation/differentiation within the APO. Recent studies screening the transcriptome and proteome of *B. glabrata* have yielded promising candidates that possess canonical domains associated with hematopoietic factors of other organisms, both invertebrate and vertebrate (12).

Granulins are evolutionarily conserved growth factors. Whereas fungi appear to lack a granulin gene (*GRN*), other members of the plant and animal kingdoms surveyed so far possess at least one copy of *GRN*. Granulins are identified by a unique 12-cysteine motif that can be found, often repeatedly, throughout the progranulin protein (PGRN). These are secreted propeptides that can be subsequently cleaved into smaller functional units by elastase (13). Progranulin is involved in numerous biological processes including tissue repair (14), early embryogenesis, inflammation,

---

Significance

Snails serve as hosts for the larval development of many medically and agriculturally important parasitic flatworms, including schistosomes, blood flukes that collectively infect more than 260 million people globally. Here, we functionally characterize a granulin-like snail growth factor that drives the development of snail immune cells, thereby making a schistosome-susceptible snail resistant to infection. This study presents the functional characterization of an endogenous gastropod growth factor as well as demonstrated reversal of a susceptible snail phenotype toward resistance using a defined snail factor.

CELL BIOLOGY

PNAS

neurobiology, and cell proliferation (15), via activation of the MAPK pathway (13). The products of PGRN cleavage (usually ∼6 kDa) can also be functional in a variety of roles that includes participation in and activation of the immune response (16).

We report on the identification and functional characterization of a progranulin molecule [*B. glabrata* granulin (*Bg*GRN)] from the snail *B. glabrata*. This study represents a number of significant advancements for the *B. glabrata*–*S. mansoni* infection model and for the field of gastropod immunobiology. We demonstrate that *Bg*GRN expression is responsive to *S. mansoni* challenge and induces the proliferation of *B. glabrata* immune cells, driving the in vivo development of an adherent hemocyte subset distinct from resident hemocytes. This effect is initiated via induction of the MAPK signaling pathway, and can be inhibited by knockdown of *Bg*GRN using RNAi as well as via preincubation with a blocking antibody. Administration of recombinant *Bg*GRN into a *B. glabrata* snail strain that is highly susceptible to *S. mansoni* infection before challenge resulted in a significant reversal of the susceptible phenotype. This study demonstrates the induction of resistance phenotype following *S. mansoni* challenge by using a defined gastropod-specific factor.

Results

In Silico Analysis of *Bg*GRN

***Bg*GRN domain prediction and comparison with schistosome granulin.** The *B. glabrata*, *Schistosoma mansoni*, *Schistosoma hematobium*, and *Schistosoma japonicum* progranulin proteins all possess multiple granulin domains (Fig. 1 *A* and *B* and Fig. S1). *B. glabrata* GRN has four predicted granulin domains characterized by amino acid residues 68–112, 158–200, 237–279, and 319–361. Modeling of *Bg*GRN suggests that it shares secondary and tertiary structural properties with known structures of human granulin A and carp granulin. Although the number of granulin domains differ between *Bg*GRN and the human and carp granulins, superimposition reveals predicted overlap of the α-helices and β-sheets associated with the conserved 12-cysteine domains (Fig. 1*C*).

Signal peptide and cleavage site annotations. *Bg*GRN has a predicted size of ∼44 kDa, and was consistently observed as a single band in Western blot of nonmanipulated snail plasma, as was recombinant *Bg*GRN (r*Bg*GRN). *S. mansoni* sporocyst ES products were not positive for GRN when probed with anti-*Bg*GRN antibody. *Bg*GRN possesses a predicted secretion signal domain in residues 1–18 (Fig. 1*B*), along with five elastase cleavage sites. Four of these sites immediately follow the four granulin domains, and the fifth cleavage site is predicted at the C-terminal end of pro-*Bg*GRN. Incubation of r*Bg*GRN with porcine elastase supports an elastase-mediated mechanism for processing of pro-*Bg*GRN, yielding two distinct ∼18- and ∼8-kDa bands that are consistent with the smaller predicted size of the *Bg*GRN cleavage products (Fig. S2). Longer elastase treatment appeared to produce more of the 8-kDa cleavage product at the expense of the larger pro-*Bg*GRN (Fig. S2). Although cleavage products at these approximate sizes were not detected by Western blot analysis of plasma isolated from non-manipulated snails, cleavage products were observed in the plasma of *S. mansoni*-challenged M-line (only ∼18-kDa product; Fig. 2*B*, *Inset*), and BS-90 (∼18- and ∼8-kDa products; Fig. 2*A*, *Inset*) and hemocyte lysates (∼18- and ∼8-kDa products; Fig. S3).

Analysis of *Bg*GRN Transcript and Protein Expression.

Quantitative RT-PCR analysis of *Bg*GRN transcript at key time points during the intramolluscan development of *S. mansoni*. The mean basal transcript abundance of *Bg*GRN as measured by specific primed (Table S1) reactions in BS-90 strain *B. glabrata* compared with M-line strain was found to be very similar following normalization to β-actin. The mean ΔCτ *Bg*GRN value in nonmanipulated BS-90 snails was 7.78 (SEM = 0.80; *n* = 5) compared with 7.46 (SEM = 0.11; *n* = 5) in M-line snails. No change in *Bg*GRN expression was observed at 1 h post challenge (hpc) with *S. mansoni* in BS-90 or M-line snails (Fig. 2); however, after 1 h, each snail strain displayed different expression

Fig. 1. In silico prediction of *Bg*GRN granulin domain architecture compared with some known and predicted granulins. (*A*) The consensus sequence of the *Bg*GRN granulin domain highlighting the canonical 12-cysteine motif that defines granulin proteins. (*B*) Reference diagram highlighting the predicted locations of the granulin domain (green arrows) in the predicted progranulin protein sequences of *B. glabrata*, *S. mansoni*, *S. hematobium*, and *S. japonicum*. Predicted signal peptides (SP) are highlighted in blue arrows and are followed by the predicted cut site (CS) for the signal peptide. Predicted elastase cleavage sites for *Bg*GRN are highlighted with a red line intersecting the protein at the approximate cut site. (*C*) The predicted 3D structure of *Bg*GRN compared with the two known crystal structures for human (*i*) and carp (*ii*) granulins, with a focus on the similar organization of β-sheets and α-helices (*iii*).

profiles. *Bg*GRN transcript abundance increased as early as 3 hpc in BS-90 snails [fold change (Rq) = 9.3, SEM = 4.77], and, by 12 hpc, *Bg*GRN abundance had increased significantly compared with control BS-90 snails (Rq = 26.8, SEM = 5.3). Highest *Bg*GRN transcript levels appeared at 1 d post challenge (dpc; Rq = 38.5, SEM = 7.88), and then decreased consistently from 2 dpc until day 35 (Rq day 2 = 17.5, SEM = 2.01; Rq day 35 = 1.05, SEM = 0.17; Fig. 2*A*). Compared with M-line snails challenged at the same time, the BS-90 snail *Bg*GRN transcript levels were significantly higher at 12 h and 1 dpc (*P* < 0.05). None of the BS-90 snails tested positive for *S. mansoni* GAPDH after 3 dpc, a result consistent with the BS-90 snails being resistant to infection with *S. mansoni* and clearing the infection within 4 d (17).

*Bg*GRN also increased in abundance following challenge of M-line *B. glabrata* with *S. mansoni* (Fig. 2*B*). Increases were observed at 3 hpc (Rq = 4.3, SEM = 1.26), peaking at 1 dpc (Rq 1 day = 15.58, SEM = 2.25). Although *Bg*GRN transcript levels declined after 1 dpc, relative expression compared with BS-90 snails remained consistently high, with a second peak in expression at day 35 (Rq day 2 = 8.32, SEM = 1.65; Rq day 35 = 11.11, SEM = 2.70). *Bg*GRN transcript abundance was significantly higher than controls at 1 and 35 dpc (*P* < 0.05). A total of 96% of the experimental M-line snails were positive for *S. mansoni* GAPDH, indicating successful infections in these snails. Plasma *Bg*GRN lagged behind transcript expression, with peak expression at 2 dpc in BS-90 and M-line snails but with earlier appearance and higher abundance in the former (Fig. 2, *Inset*).

Plasma *Bg*GRN in *B. glabrata* before and after siRNA-mediated knockdown. In both snail strains, injection of *Bg*GRN-specific siRNA oligos (Table S1) effectively knocked down *Bg*GRN expression,
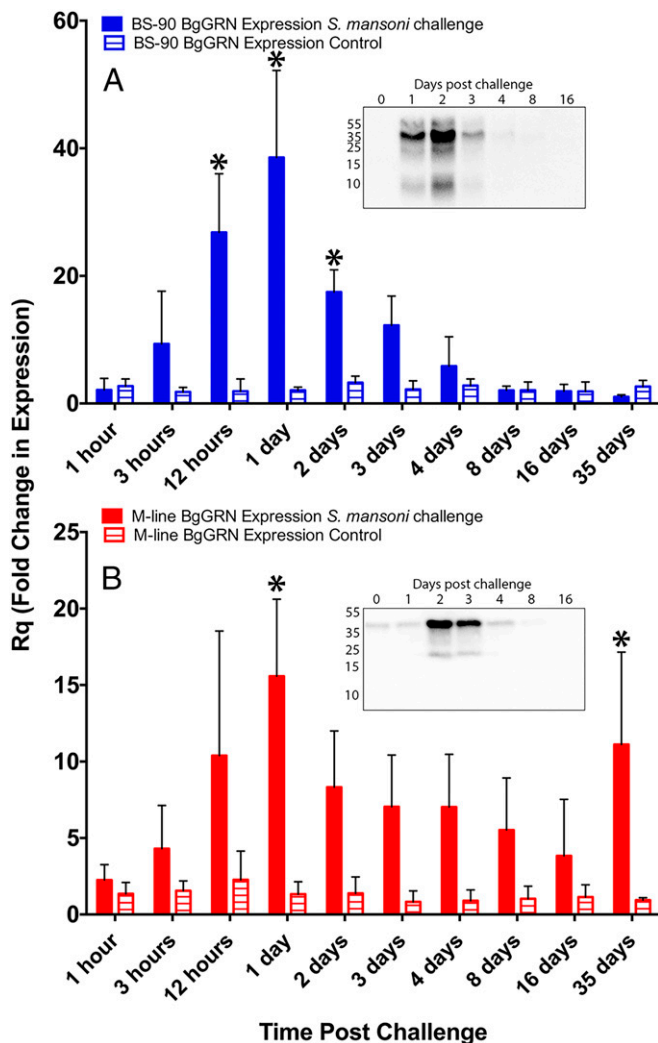
Fig. 2. Quantitative RT-PCR (qRT-PCR) analysis of *Bg*GRN expression in M-line and BS-90 strains of *B. glabrata* at critical time points during the entire intramolluscan development of *S. mansoni*. Fold change of *Bg*GRN expression in BS-90 (*A*; blue bars; $n = 3$ for each time point) and M-line (*B*; red bars; $n = 5$ for each time point) strains challenged with *S. mansoni* (full bars) or, not-challenged control (hatched bars) following normalization to a time 0 control group ($n = 5$ snails) and then to the endogenous control β-actin. Bars represent SE. Asterisks represent within-strain significant difference between *S. mansoni*-challenged and not-challenged snails at the specific time point ($P < 0.05$). (*Insets*) Western blot analyses of *S. mansoni*-challenged snail plasma at the indicated days post challenge.

thereby reducing endogenous *Bg*GRN (Fig. S4). Knockdown impact on plasma *Bg*GRN was noticeable by 2 d post injection, with almost complete loss of detectable *Bg*GRN by 5 d post injection. Knockdown of *Bg*GRN 4 d before challenge with *S. mansoni* resulted in an almost complete abrogation of any challenge-mediated induction of *Bg*GRN expression in BS-90 snails compared with GFP-knockdown controls (Fig. S4).

BgGRN Induces Proliferation of Hemocytes and B. glabrata Embryonic Cells in Vivo and in Vitro via ERK Pathway Signaling. Coinjection of BrdU with rBgGRN into BS-90 snails resulted in an increased percentage of circulating hemocytes positive for BrdU (BrdU+) after 48 h compared with vehicle controls of medium alone (Fig. 3). The mean baseline percentage of BrdU+ circulating hemocytes in BS-90 snails was found to be 17.9% (SEM = 1.4%), compared with 19.8% (SEM = 1.3%), 28% (SEM = 1.6%), 34% (SEM = 2.1%), and 40.1% (SEM = 1.8%) BrdU+ hemocytes following 48 h

stimulation with 25, 50, 100, and 200 nM *Bg*GRN, respectively. Natural levels of circulating *Bg*GRN observed in snail plasma (12.1 ± 3.67 nM) increased as a result of *S. mansoni* challenge in BS-90 snails to a peak of 110.3 ± 16.3 nM at day 2 post challenge. Circulating *Bg*GRN returned to baseline concentrations (13.4 ± 3.76 nM) by day 8 post challenge (Fig. S5). The percentage of cells that had incorporated BrdU following *Bg*GRN injection was comparable to the positive control phorbol 12-myristate 13-acetate (PMA), in which 24% (SEM = 1.2%), 29% (SEM = 1.5%), and 38.3% (SEM = 2.1%) of circulating hemocytes were positive for BrdU after injection of 100, 200, and 300 nM PMA, respectively. Inhibition of the ERK signaling pathway by U0126 at a concentration of 10 μM abrogated *Bg*GRN and PMA-induced proliferation (i.e., BrdU incorporation) in circulating hemocytes (Fig. 3).

*Bg*GRN elicited very similar results when applied to *B. glabrata* embryonic (Bge) cells ($n = 6$ for all treatments) for 48 h under in vitro culture conditions (Fig. S6). The mean percentage of BrdU+ Bge cells cultured in medium alone was 26% (SEM = 1.2%), compared with 32.8% (SEM = 1.4%), 39% (SEM = 1.1%), 43.8% (SEM = 1.3%), and 44.9% (SEM = 0.8%) after treatment with 25, 50, 100, and 200 nM *Bg*GRN. BrdU was incorporated into the DNA of 31.7% (SEM = 1.0%), 35.1% (SEM = 1.5%), and 43.4% (SEM = 1.3%) of Bge cells following treatment with PMA at concentrations of 100, 200, and 300 nM. As with primary hemocytes, the proliferation induced by *Bg*GRN and PMA was abrogated by application of 10 μM U0126.

Knockdown of *Bg*GRN in BS-90 and Bge cells 4 d before assessment of BrdU incorporation resulted in a nonsignificant, but observable, reduction of BrdU+ cells in both groups [14.7% (SEM = 0.9%)]
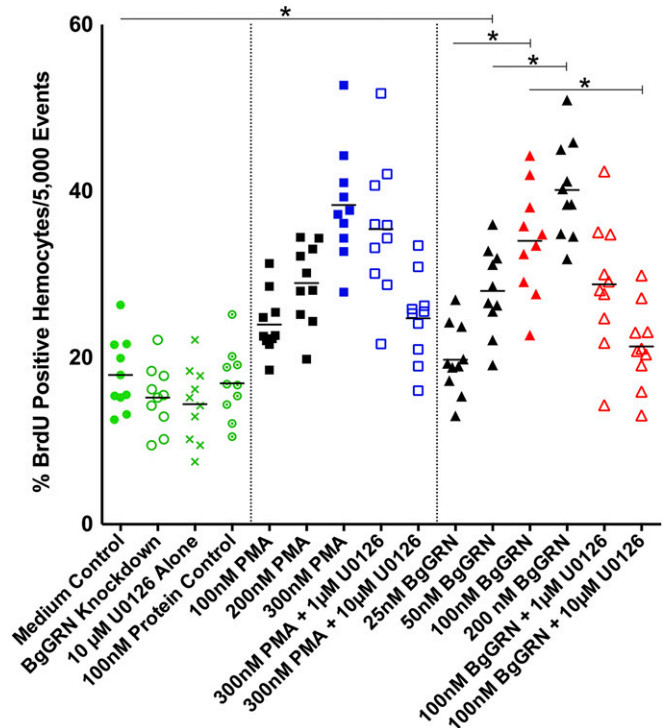

Fig. 3. *Bg*GRN-induced proliferation of circulating BS-90 *B. glabrata* hemocytes in vivo. Measurement of the percent BrdU-positive BS-90 primary hemocytes (out of 5,000 total events; $n = 10$ independent trials for each treatment) following 48 h stimulation. Exposures to 25, 50, 100, and 200 nM rBgGRN were compared with 100, 200, and 300 nM PMA (positive controls) and negative controls (medium, knockdown, recombinant protein, and inhibitor-only controls). Increases in the percentage of BrdU-positive cells were rBgGRN dose-dependent, with an apparent plateau at 100 nM. Important comparisons of significance are highlighted and indicated by asterisks.

CELL BIOLOGY

and [23.3% (SEM = 1.0%), respectively] compared with controls (as detailed earlier; Fig. 3 and Fig. S6). Assessment of newly proliferated hemocytes using *B. glabrata* fibrinogen-related protein 3 (*Bg*FREP3) (2) and *Bg* Toll-like receptor (*Bg*TLR) (18)—proteins known to be associated with resistance to *S. mansoni*—indicates that *Bg*GRN-induced hemocytes have a higher percentage of *Bg*TLR-positive cells whereas the proportion of *Bg*FREP3-positive cells was unaffected (Fig. S7).

Western blot analysis confirmed that induction of cellular proliferation by *Bg*GRN occurred, in part, via phosphorylation of the p44/42 MAPK in the ERK signaling pathway (Fig. S8). Injection of 100 nM rBgGRN into BS-90 snails resulted in phosphorylation of ERK1/2 at 15 min post injection, with maximal phosphorylated ERK compared with total ERK observed at 30 and 60 min post induction. At 90, 120, and 240 min post treatment, the amount of phosphorylated ERK declined, but remained detectable. Total ERK levels remained constant. As with other assessments of *B. glabrata* ERK1/2 analyses by Western blot, only a single band was easily visible in our experiments (19).

BgGRN Stimulates Generation of Adherent Hemocytes in Vivo. The baseline number of adherent (spread) hemocytes in BS-90 snails was more than double the mean number in M-line snails (171.5; SEM = 7.3; $n = 30$; and 83.7; SEM = 3.8; $n = 30$, respectively; Fig. 4*A*). Injection of rBgGRN to a final concentration of ~100 nM in the snail hemolymph 48 h before hemocyte isolation significantly increased the number of adherent hemocytes isolated from both snails [BS-90 = 216.5; SEM = 8.9 ($n = 30$), M-line = 158.4; SEM = 7.5 ($n = 30$)]. These values reflect 126% and 189% increases in the number of circulating hemocytes in BS-90 and M-line snails, respectively, increasing the number of adherent hemocytes in the M-line snails such that there was no statistically significant difference between the baseline BS-90 and M-line + rBgGRN groups. We confirmed that the increase in adherent hemocytes was the direct result of *Bg*GRN-induced proliferation by enumerating BrdU+ adherent hemocytes following *Bg*GRN injection in snails (Fig. S9). Preincubation of rBgGRN with a polyclonal αBgGRN antibody blocked the increase in adherent cell numbers, confirming that the proliferative effect was the result of application of rBgGRN (Fig. 4*A*).

Knockdown of *Bg*GRN significantly reduced the number of adherent hemocytes in BS-90 [130.8 (SEM = 6.0)], but not in M-line [76.3 (SEM = 3.1)], snails compared with GFP-specific knockdown controls (BS-90 = 176.2; SEM = 5.5; M-line = 89.1; SEM = 4.1; Fig. 4*A*). No significant changes in adherent hemocyte numbers isolated from BS-90 or M-line snails were measured following treatment with 100 nM recombinant protein control (*Bg*Temptin produced in same expression system) or a polyclonal mouse-derived isotype control (αHSP70).

Prior Stimulation of Hemocyte Proliferation by BgGRN in Naturally Susceptible B. glabrata Snails Significantly Protects Against S. mansoni Infection. Significantly fewer M-line snails injected with rBgGRN, before exposure to *S. mansoni*, developed patent infections compared with snails injected with a recombinant protein control (Fig. 4*B*). This trend was observed throughout the course of the intramolluscan infection. The percentages of the experimental snail group ($n = 100$) that shed *S. mansoni* cercariae were 0%, 14%, 30%, 34%, and 32% at weeks 4, 5, 6, 7, and 8, respectively. In contrast, 2%, 59%, 80%, 88%, and 84% of the control snails ($n = 50$) shed cercariae at the same time post challenge. The percentage of infected snails was significantly different between rBgGRN-injected M-line snails and those injected with the recombinant protein control from week 5 post challenge onward (Fig. 4*B*). Sporocysts were not found in any of the M-line snails that did not shed cercariae. The knockdown of *Bg*GRN in BS-90 snails had a small impact on *S. mansoni* challenge outcome: 6%, 10%, and 11% shed *S. mansoni* cercariae on weeks 6, 7, and 8, respectively ($n = 100$), whereas none of the GFP-knockdown controls shed cercariae at any point ($n = 50$; Fig. 4*B*).
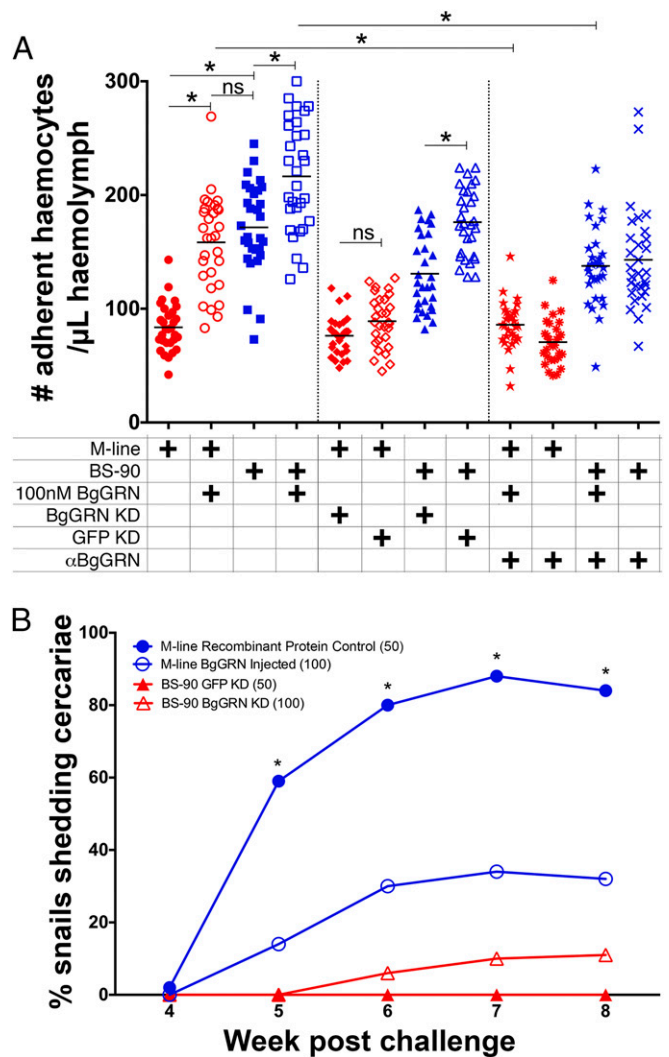

Fig. 4. *Bg*GRN induces the proliferation and development of adherent hemocytes to the point that susceptible M-line *B. glabrata* are able to defend against *S. mansoni* infection. (*A*) Effects of rBgGRN, knockdown of *Bg*GRN, and anti-*Bg*GRN polyclonal antibody on the number of adherent hemocytes. Snails were injected with 100 nM rBgGRN (induction) or rBgGRN preincubated with anti-*Bg*GRN antibody (abrogation treatment), and, 48 h later, hemocytes were isolated and used for adherent hemocyte counts. Knockdown snails received siRNA oligos against *Bg*GRN or GFP (control) 48 h before the treatments. Important comparisons of significance are highlighted and indicated by asterisks. (*B*) Injection of rBgGRN into M-line *B. glabrata* 4 d before challenge with *S. mansoni* significantly impacted *S. mansoni* infection success. Complementary knockdown of *Bg*GRN in BS-90 *B. glabrata* also altered *S. mansoni* infection success rate, albeit not significantly.

Discussion

Encapsulation of schistosome sporocysts by snail hemocytes is critical for the elimination of the parasite (5, 10). This highlights the importance of maintaining a sufficient population of readily mobilized hemocytes within a snail at all times, and also the ability to drive production of new cells rapidly in response to challenge. The results of this study demonstrate that *Bg*GRN participates in the hematopoietic events that control the production of the circulating hemocyte population. Introduction of *Bg*GRN into *B. glabrata* snails that are naturally susceptible to *S. mansoni* infection resulted in a 54% reduction in the number of snails successfully infected by week 7 post challenge. That sporocysts were not observed upon dissection of these refractory M-line snails implies that the snails had successfully

cleared any parasites. Underpinning this impressive change in infection outcome is a significant increase in the generation of circulating adherent hemocytes, which is the hemocyte subset that participates in the encapsulation of *S. mansoni* sporocysts (10). Adherent hemocytes are also highly phagocytic (2) and are responsible for the production of reactive and nitrogen intermediates (11) and soluble immune factors that are important for successful clearance of digenetic trematodes (1, 2). This cell population nearly doubled following administration of rBgGRN.

Whether the snails in this study defended against infection by *S. mansoni* because they had higher circulating cell numbers, or because those additional cells were immunologically distinct and conveyed new immune functionality, is a central question. To address it, we used two known immunological markers of snail resistance to *S. mansoni* infection: *Bg*FREP3 (3) and *Bg*TLR (18). That *Bg*TLR was found to be proportionally higher on BrdU-positive cells induced by *Bg*GRN, and *Bg*FREP3 was not, suggests that the hemocyte population induced by *Bg*GRN may be more geared toward the cellular immune response than the humoral. Increase in the *Bg*GRN-induced adherent hemocyte numbers in the susceptible M-line strain of *B. glabrata* paralleled the mean number of hemocytes present in the naturally refractory BS-90 strain before stimulation. These findings support the hypothesis that *B. glabrata* resistance to *S. mansoni* infection is influenced by the hemocyte numbers and repertoire of the snail (5).

*Bg*GRN possesses five predicted elastase cleavage sites that are each located immediately following one of the four 12-cysteine granulin domains. Similar to observations that have been made in studies focusing on human PGRN (16), incubation of rBgGRN with elastase results in the production of ~8-kDa granulin fragments that would be predicted should all cleavage sites be processed; at least one intermediate product is consistently present in *Bg*GRN elastase digests that resides at ~18 kDa, similar in size to the ~15-kDa intermediate fragment observed when human PGRN is digested with elastase (16). As porcine elastase was used to cleave rBgGRN, it is possible that differences between porcine elastase and the elastase of *B. glabrata* underpin the cleavage patterns observed. *B. glabrata* elastases were found to possess catalytic sites known to be active in human and porcine elastases ([Fig. S10](#)), indicating that they do possess the canonical motifs relevant for traditional elastase function (20). However, two of the three *B. glabrata* elastase variants found had only incomplete sequences available, and, consequently, the final catalytic residue could not be compared.

Native *Bg*GRN was detectable in the plasma of unexposed *B. glabrata* only in its progranulin form; the ~18-kDa cleavage product was observed only in plasma (of both M-line and BS-90 snails) following *S. mansoni* challenge, and the ~8-kDa product was seen only in BS-90 plasma following challenge. In addition, the intermediate ~18-kDa and smaller ~8-kDa fragments were observed in the cytoplasmic fractions of *B. glabrata* hemocyte lysates. These observations suggest that activation or stimulation of the hemocytes (or other *Bg*GRN producing cells) leads to the cleavage of *Bg*GRN. These observations are supported by studies demonstrating that, in some cases, cleavage of PGRN by enzymes such as matrix metalloproteinase-12 occurs within the cytoplasm (21). Whether the cytoplasmic *Bg*GRN and observed fragments differ functionally from extracellular *Bg*GRN remains unknown. The source of the cytoplasmic *Bg*GRN, which could derive from extracellular *Bg*GRN that enters hemocytes or posttranslational processing of *Bg*GRN before secretion, remains to be determined.

Although the hemocyte receptor mediating the proliferative effects of *Bg*GRN observed in this study is unknown, there are a number of candidate receptors that warrant investigation. Even within the mammalian PGRN literature, there remains uncertainty regarding a definitive GRN receptor. Sortilin (22) and TNF receptors (23) have been implicated in recognition of PGRN, although recent evidence contradicts these initial reports (24). TLR9

activation has also been found to be reliant on PGRN as a cofactor (25). At present, we know very little about whether homologs of these molecules exist in *B. glabrata*. Analysis of the *B. glabrata* genome highlights the presence of genes that possess high predicted amino acid identity to the canonical domains that characterize TNF receptors and sortilin. However, whether these genes are expressed, or encode for proteins that function in a similar manner to known mammalian molecules, has not yet been investigated to our knowledge. Of the possible candidate molecules that may interact with *Bg*GRN, TLRs are the best characterized in *B. glabrata*. A number of leucine-rich repeat domain-containing transcripts have been identified in the *B. glabrata* genome, and at least 13 of these appear to be bona fide TLRs possessing a toll-interleukin-1 domain. Although little is known about the functions of these TLRs, the fact that *B. glabrata* possesses many of the downstream components associated with TLR signaling in other organisms (26), and that at least one TLR in *B. glabrata* is highly abundant on *Bg*GRN-induced adherent hemocytes, is indicative that they likely retain their role as pattern-recognition receptors in *B. glabrata* and are important participants in the immune response.

Although the receptor for *Bg*GRN may remain unknown, it appears that the effects of *Bg*GRN are mediated by signaling via the MAPK pathway and ERK1/2. The signaling pathway used by PGRN appears to be a highly conserved aspect of its biology (15). This is noteworthy, as it has been demonstrated that *S. mansoni* is able to interfere with the phosphorylation of ERK1/2 in susceptible snails, but not those that are phenotypically resistant (19). The kinetics of ERK1/2 phosphorylation following rBgGRN stimulation of hemocytes has also been observed by using human recombinant PGRN (27); however, phosphorylated ERK1/2 is detectable for a longer time (4 h vs. ~2 h).

The 12-cysteine motif that characterizes granulins defines the protein and confers its conserved secondary and tertiary structure. It may also be responsible for certain functions (28). Investigations in carp identified three isoforms of carp GRN (29) that were later associated with mononuclear phagocytes (30). Functional studies of the carp granulin homolog in the goldfish demonstrated that this teleost granulin shares hematopoietic functions with its mammalian counterparts, inducing proliferation of myeloid cells in vitro (31). Recent studies focusing on a PGRN produced by the flatworm parasite *Opisthorchis viverrini* demonstrate *Ov*GRN can induce proliferation in fibroblasts of the parasite's human host and fibroblast cell lines, thereby providing a plausible mechanism for the high rates of liver cancer in individuals infected by *O. viverrini* (32, 33). The *Ov*GRN studies provide plausibility for a functional role of parasite GRNs on certain host tissues or, alternatively, host GRNs on certain parasite tissues, and highlight the functional and structural conservation of granulins.

The variety of biological functions that PGRN is capable of is impressive, and it is likely that *Bg*GRN may also participate in wound healing, immunological defense, and neuronal development in *B. glabrata*. Despite its pleiotropic function, we have demonstrated that *Bg*GRN is an important growth factor in *B. glabrata*, driving hemocyte proliferation and development of an adherent hemocyte subset that is central to the defense of the snail against *S. mansoni*. Although the list of factors and genes that influence compatibility between *B. glabrata* and *S. mansoni* continues to grow, we demonstrate in this study that hematopoietic events regulated by endogenous factors such as granulin can significantly impact the outcome of *S. mansoni* infection, and that not all hemocytes are equal when considering their role in the immune response.

Materials and Methods

Additional description of materials and methods is provided in *SI Materials and Methods*.

Snail and Bge Cell Culture and Maintenance. The M-line and BS-90 strains of the snail *B. glabrata* are susceptible and refractory to infection with *S. mansoni*,

CELL BIOLOGY

respectively. Both snail populations are maintained in colonies at the University of Alberta as previously described (34). The Bge cell line (35) (American Type Culture Collection NR-21959) was maintained in Bge cell medium by using established protocols (36).

Anti-*Bg*GRN Polyclonal Antibody Generation and Validation. A mouse anti-*Bg*GRN polyclonal antibody was generated against the recombinant *Bg*GRN (GenScript). The antibody was affinity purified using a Protein G affinity column (no. 17–0404-01; GE Healthcare) and then further purified against recombinant *Bg*GRN. It was effective for Western blot detection of native *Bg*GRN at concentrations of 1:5,000, and was found to block the proliferation-inducing effects of rBgGRN at concentrations of 1:250. All protocols involving animals were carried out in accordance with the Canadian Council on Animal Care Guidelines and Policies with approval from the Animal Care and Use Committee (Biosciences) for the University of Alberta AUP00000057.

1. Galinier R, et al. (2013) Biomphalysin, a new β pore-forming toxin involved in Biomphalaria glabrata immune defense against Schistosoma mansoni. *PLoS Pathog* 9(3): e1003216.
2. Hanington PC, et al. (2010) Role for a somatically diversified lectin in resistance of an invertebrate to parasite infection. *Proc Natl Acad Sci USA* 107(49):21087–21092.
3. Moné Y, et al. (2010) A large repertoire of parasite epitopes matched by a large repertoire of host immune receptors in an invertebrate host/parasite model. *PLoS Negl Trop Dis* 4(9):e813.
4. Baeza Garcia A, et al. (2010) Involvement of the cytokine MIF in the snail host immune response to the parasite Schistosoma mansoni. *PLoS Pathog* 6(9):e1001115.
5. Larson MK, Bender RC, Bayne CJ (2014) Resistance of Biomphalaria glabrata 13-16-R1 snails to Schistosoma mansoni PR1 is a function of haemocyte abundance and constitutive levels of specific transcripts in haemocytes. *Int J Parasitol* 44(6):343–353.
6. Jeong KH, Lie KJ, Heyneman D (1983) The ultrastructure of the amebocyte-producing organ in Biomphalaria glabrata. *Dev Comp Immunol* 7(2):217–228.
7. Sullivan JT, Pikios SS, Alonzo AQ (2004) Mitotic responses to extracts of miracidia and cercariae of Schistosoma mansoni in the amebocyte-producing organ of the snail intermediate host Biomphalaria glabrata. *J Parasitol* 90(1):92–96.
8. Noda S (1992) Effects of excretory-secretory products of Echinostoma paraensei larvae on the hematopoietic organ of M-line Biomphalaria glabrata snails. *J Parasitol* 78(3): 512–517.
9. Lie JK, Heyneman D, Jeong KH (1976) Studies on resistance in snails. 4. Induction of ventricular capsules and changes in the amebocyte-producing organ during sensitization of Biomphalaria glabrata snails. *J Parasitol* 62(2):286–291.
10. LoVerde PT, Shoulberg N, Gherson J (1984) Role of cellular and humoral components in the encapsulation response of Biomphalaria glabrata to Schistosoma mansoni sporocysts in vitro. *Prog Clin Biol Res* 157:17–29.
11. Humphries JE, Yoshino TP (2008) Regulation of hydrogen peroxide release in circulating hemocytes of the planorbid snail Biomphalaria glabrata. *Dev Comp Immunol* 32(5):554–562.
12. Hanington PC, Lun CM, Adema CM, Loker ES (2010) Time series analysis of the transcriptional responses of Biomphalaria glabrata throughout the course of intramolluscan development of Schistosoma mansoni and Echinostoma paraensei. *Int J Parasitol* 40(7):819–831.
13. Zanocco-Marani T, et al. (1999) Biological activities and signaling pathways of the granulin/epithelin precursor. *Cancer Res* 59(20):5331–5340.
14. He Z, Bateman A (2003) Progranulin (granulin-epithelin precursor, PC-cell-derived growth factor, acrogranin) mediates tissue repair and tumorigenesis. *J Mol Med (Berl)* 81(10):600–612.
15. Ong CH, Bateman A (2003) Progranulin (granulin-epithelin precursor, PC-cell derived growth factor, acrogranin) in proliferation and tumorigenesis. *Histol Histopathol* 18(4):1275–1288.
16. Zhu J, et al. (2002) Conversion of proepithelin to epithelins: Roles of SLPI and elastase in host defense and wound repair. *Cell* 111(6):867–878.
17. Sullivan JT, Spence JV, Nuñez JK (1995) Killing of Schistosoma mansoni sporocysts in Biomphalaria glabrata implanted with amoebocyte-producing organ allografts from resistant snails. *J Parasitol* 81(5):829–833.
18. Pila EA, Tarrabain M, Kabore AL, Hanington PC (2016) A novel Toll-like receptor (TLR) influences compatibility between the gastropod Biomphalaria glabrata, and the digenean trematode Schistosoma mansoni. *PLoS Pathog* 12(3):e1005513.
19. Zahoor Z, Davies AJ, Kirk RS, Rollinson D, Walker AJ (2008) Disruption of ERK signalling in Biomphalaria glabrata defence cells by Schistosoma mansoni: Implications for parasite survival in the snail host. *Dev Comp Immunol* 32(12):1561–1571.
20. Korkmaz B, Horwitz MS, Jenne DE, Gauthier F (2010) Neutrophil elastase, proteinase 3, and cathepsin G as therapeutic targets in human diseases. *Pharmacol Rev* 62(4): 726–759.
21. Suh HS, Choi N, Tarassishin L, Lee SC (2012) Regulation of progranulin expression in human microglia and proteolysis of progranulin by matrix metalloproteinase-12 (MMP-12). *PLoS One* 7(4):e35115.
22. Zheng Y, Brady OA, Meng PS, Mao Y, Hu F (2011) C-terminus of progranulin interacts with the beta-propeller region of sortilin to regulate progranulin trafficking. *PLoS One* 6(6):e21023.
23. Jian J, et al. (2013) Progranulin directly binds to the CRD2 and CRD3 of TNFR extracellular domains. *FEBS Lett* 587(21):3428–3436.
24. Chen X, et al. (2013) Progranulin does not bind tumor necrosis factor (TNF) receptors and is not a direct regulator of TNF-dependent signaling or bioactivity in immune or neuronal cells. *J Neurosci* 33(21):9202–9213.
25. Moresco EM, Beutler B (2011) Special delivery: Granulin brings CpG DNA to Toll-like receptor 9. *Immunity* 34(4):453–455.
26. Zhang SM, Coultas KA (2011) Identification and characterization of five transcription factors that are associated with evolutionarily conserved immune signaling pathways in the schistosome-transmitting snail Biomphalaria glabrata. *Mol Immunol* 48(15-16): 1868–1881.
27. Monami G, et al. (2006) Proepithelin promotes migration and invasion of 5637 bladder cancer cells through the activation of ERK1/2 and the formation of a paxillin/FAK/ERK complex. *Cancer Res* 66(14):7103–7110.
28. Bateman A, Bennett HP (2009) The granulin gene family: From cancer to dementia. *BioEssays* 31(11):1245–1254.
29. Belcourt DR, Lazure C, Bennett HP (1993) Isolation and primary structure of the three major forms of granulin-like peptides from hematopoietic tissues of a teleost fish (Cyprinus carpio). *J Biol Chem* 268(13):9230–9237.
30. Belcourt DR, Okawara Y, Fryer JN, Bennett HP (1995) Immunocytochemical localization of granulin-1 to mononuclear phagocytic cells of the teleost fish Cyprinus carpio and Carassius auratus. *J Leukoc Biol* 57(1):94–100.
31. Hanington PC, Barreda DR, Belosevic M (2006) A novel hematopoietic granulin induces proliferation of goldfish (Carassius auratus L.) macrophages. *J Biol Chem* 281(15):9963–9970.
32. Smout MJ, et al. (2009) A granulin-like growth factor secreted by the carcinogenic liver fluke, Opisthorchis viverrini, promotes proliferation of host cells. *PLoS Pathog* 5(10):e1000611.
33. Papatpremsiri A, et al. (2015) Suppression of Ov-grn-1 encoding granulin of Opisthorchis viverrini inhibits proliferation of biliary epithelial cells. *Exp Parasitol* 148:17–23.
34. Stibbs HH, Owczarzak A, Bayne CJ, DeWan P (1979) Schistosome sporocyst-killing Amoebae isolated from Biomphalaria glabrata. *J Invertebr Pathol* 33(2):159–170.
35. Hansen EL (1976) A cell line from embryos of Biomphalaria glabrata (Pulmonata): Establishment and characteristics. *Invertebrate Tissue Culture: Research Applications*, 1-393 (Academic, New York), pp 75–99.
36. Yoshino TP, Bickham U, Bayne CJ (2013) Molluscan cells in culture: Primary cell cultures and cell lines. *Can J Zool* 91(6):391–404.
37. Adema CM, et al. (2010) Differential transcriptomic responses of Biomphalaria glabrata (Gastropoda, Mollusca) to bacteria and metazoan parasites, Schistosoma mansoni and Echinostoma paraensei (Digenea, Platyhelminthes). *Mol Immunol* 47(4): 849–860.
38. Ulmer MJ (1970) Notes on rearing of snails in the laboratory. *Experiments and Techniques in Parasitology* (W. H. Freeman., San Francisco), pp 143–144.
39. Petersen TN, Brunak S, von Heijne G, Nielsen H (2011) SignalP 4.0: Discriminating signal peptides from transmembrane regions. *Nat Methods* 8(10):785–786.
40. Emanuelsson O, Nielsen H, Brunak S, von Heijne G (2000) Predicting subcellular localization of proteins based on their N-terminal amino acid sequence. *J Mol Biol* 300(4):1005–1016.
41. Nielsen H, Engelbrecht J, Brunak S, von Heijne G (1997) Identification of prokaryotic and eukaryotic signal peptides and prediction of their cleavage sites. *Protein Eng* 10(1):1–6.
42. Käll L, Krogh A, Sonnhammer EL (2007) Advantages of combined transmembrane topology and signal peptide prediction–the Phobius web server. *Nucleic Acids Res* 35(Web server issue):W429–432.
43. Finn RD, et al. (2014) Pfam: The protein families database. *Nucleic Acids Res* 42(database issue):D222–D230.
44. Kim DE, Chivian D, Baker D (2004) Protein structure prediction and analysis using the Robetta server. *Nucleic Acids Res* 32(Web server issue):W526–531.
45. Berman HM, et al. (2000) The Protein Data Bank. *Nucleic Acids Res* 28(1):235–242.
46. Boyle JP, Wu XJ, Shoemaker CB, Yoshino TP (2003) Using RNA interference to manipulate endogenous gene expression in Schistosoma mansoni sporocysts. *Mol Biochem Parasitol* 128(2):205–215.
47. Adema CM, van Deutekom-Mulder EC, van der Knaap WP, Sminia T (1993) NADPH-oxidase activity: The probable source of reactive oxygen intermediate generation in hemocytes of the gastropod Lymnaea stagnalis. *J Leukoc Biol* 54(5):379–383.
48. Sminia T, Barendsen L (1980) A comparative morphological and enzyme histochemical study on blood-cells of the fresh-water snails Lymnaea-stagnalis, Biomphalaria-glabrata, and Bulinus-truncatus. *J Morphol* 165(1):31–39.
49. Chernin E (1963) Observations on hearts explanted in vitro from the snail Australorbis glabratus. *J Parasitol* 49(3):353–364.